Performance Evaluation of the Second Order Digital Data-Aided Loop

Tien M. Nguyen

Jet Propulsion Laboratory
California Institute of "technology
4800 Oak Grove Drive
Pasadena, CA 91109

Abstract

Performance of the second order digital Data-Aided Loop (DAL) is evaluated. The loop tracking phase jitter is determined using the current available analog results. To utilize the analog results, both Impulse Invariant Transformation (IIT) and Linear Interpolation Transformation (LIT) techniques are used in the approximation of the digital loop filter. The analytical results obtained from these transformation methods will be compared with the computer simulation results. The comparison shows that the analytical results obtained by LIT method are in good agreement with computer simulation results and hence, it can be used to predict the performance of the digital DAL,

In addition, the paper will also investigate the impact of the tracking phase jitter on the Bit Error Rate (BER) performance of the second order digital DAL, and the results are then compared with the commonly used Costas loops, namely, Costas loop with matched filter and clock feed back in the arm filter and Costas loop with second order Butterworth filter in the arm filter. The analytical results demonstrate the superiority performance of the digital DAL.

1. Introduction

In the past, the analog Data-Aided Loop (DAL) has been proposed for space applications [1, 2]. The DAL can be employed by both suppressed carrier or residual carrier communication systems. For space applications, the residual carrier systems usually use the subcarrier to separate the data from the residual carrier [3]. Basically, the DAL uses the power in the composite received signal sidebands to enhance the Signal-to-Noise Ratio (SNR) in the bandwidth of the carrier (or subcarrier) tracking. The composite received signal used in the DAL can consist of the carrier and data, or carrier and data modulated subcarrier for suppressed or residual carrier system, respectively [2]. Furthermore, for residual carrier systems, the DAL can also be used for subcarrier tracking where the composite received signal is subcarrier and data [3, Chapters 5-6].

Because of the advance in digital signal processing technology, the DAL can be easily implemented in a single Digital Signal Processing (DSP) chip. This has motivated the use of the digital DAL. for space applications where the subcarrier tracking is required to be done with a great accuracy. Figure 1 shows a simplified block diagram of the digital DAL. The digital loop filter, F(z), shown in this figure is of the second order type, hence the name second order digital DAL.

The performance of the first and second order analog DAL has been analyzed thoroughly by Simon and Springett [2]. However, the results for the second order

loop are only applicable to the second order analog loop filter, This paper attempts to use the current available results provided in [2] to derive the tracking phase jitter for the second order digital DAL, and assesses the impact of this phase jitter on the Bit Error Rate (BER) performance. The results of the phase jitter obtained by the computer simulation for the digital DAL will also be presented and compared with the theoretical results. The computer simulation has been built using the Signal Processing Worksystem (SPW) software of Comdisco Systems Inc. Furthermore, the BER performance for systems using DAL will be compared against those employing Costas loops.

The paper is organized as follows: it begins with with Section 2 where a description of the digital DAL and current available results for the second order analog DAL, To utilize the analog results, the equivalent digital loop filter in the analog domain (S-domain) is derived. 130th Impulse Invariant Transformation (IIT) and linear interpolation transformation (LIT) methods are used in the approximation of the second order digital filter in the S-domain. A mathematical model for the tracking phase jitter of the second order digital DAL is determined using the approximated filter in the S-domain. Next, in Section 4, the impact of the tracking phase jitter on the bit error rate performance of the digital DAL and Costas loops is investigated. " Costas loops with matched filter and second order Butterworth filter in the arm filter are considered here. Numerical results are presented in Section 5 using the actual design parameters for deep space missions, and the results between the digital DAL and Costas loops are compared against each other. Finally, the main conclusion is shown in Section 6.

2. Description of the Digital DAL

The input signal to the loop can be considered at baseband. This baseband signal is just the phase of the carrier at the instant of the error sample. Thus, the digital DAL block diagram shown in Figure 1 is just the phase diagram, i.e., the block diagram for processing the received phase. The sample-and-hold is triggered by the output of the Digital Controlled Oscillator (DCO). The loop is trying to sample at the zero crossing of the input sinusoid. If the error in detecting the zero crossing is ϕ and the peak amplitude is A, the data modulation is then the output of the sample-and-hold which is $Ad(t)\sin(\$)$, where d(t) is the NRZ binary data. The Analog-to-Digital Converter (ADC) convert this output into a digital data stream and this data stream is then accumulated by the error accumulator. The error accumulator is accumulated the incomming data stream over N samples per bit. N is the data rate dependent number samples. Thus, the output of the error accumulator is the sum over one bit period. This output is then multiplied by the estimate of the incoming data stream. The data-aided loop uses the data estimate to improve the tracking performance. In order to keep the loop performance the same for all data rate, the output of the multiplier is scaled by a data rate dependent constant. The scaled error signal is then smoothed by the second order filter. The error signal is used to control the output of the DCO. The DCO issues the zero crossing sample time command after counting a certain number of clock cycles based on the incoming frequency. When a correction count is received from the loop filter, the DCO adjusts its count accordingly, to advance or retard the sampling phase,

The objective of this paper is to derive the tracking phase jitter of the second order digital DAL described in Figure 1 and to assess the impact of this phase jitter on the Bit error Rate (BER) performance. Based on the available results derived for analog DAL, the following section will derive the tracking phase jitter of the second order digital DAL.

3. Tracking Phase Jitter for the Second Order Digital DAL

3.1. Current Results for the Second Order Analog DAL

A simplified block diagram for the analog DAL is shown in Figure 2. This loop has been analyzed in [1-2]. For the second order DAL, the loop filter F(s) is given by

$$F(s) = \frac{1 + s\tau_2}{1 + s\tau_1} \tag{1}$$

where τ_1 and τ_2 are the time constants of the second order loop filter. When the Loop Signal-to-Noise Ratio (LSNR) is large and the bit SNR is greater than 4 dB with the tracking phase jitter less than 15°, the variance of the tracking phase jitter can be shown to have the following form [2]

$$\sigma_\phi^2 = \left| \frac{1 + \frac{1 - F_1}{r}}{(\frac{1+r}{r})\rho} \right| \tag{2}$$

where F_1 is defined as the time constant τ_2-to-τ_1 ratio, i.e,

$$F_1 = \frac{\tau_2}{\tau_1} \tag{3}$$

and the parameter r is given by

$$r = \sqrt{P_D} K \tau_2 F_1 erf(\sqrt{R_s}), \tag{4}$$

the parameters P_D and R, denote the total received signal power and Bit SNR (BSNR), respectively, and K in Eq. *(4)* denotes the loop gain,

$$K = \frac{4}{\sqrt{P_D}\delta T_b erf(\sqrt{R_s})} \tag{5}$$

the parameter δ in Eq. (5) indicates the inverse of the product of loop bandwidth (BJ and bit period T_b, i.e.,

$$\delta = \frac{1}{B_L T_b}. \tag{6}$$

and, finally, the parameter p in Eq. (3) is given by

$$\rho = R_s \delta erf^2(\sqrt{R_s}), \tag{7}$$

Note that Eq. (2) represents the linear approximation of the tracking phase jitter for the second order loop at high bit SNR and small phase jitter error. For large r, the phase jitter described by Eq. (2) will approach (l/p), which is the phase jitter for the linear first order loop. Thus, for large r, the parameter p becomes the loop SNR.

In this paper, one is interested in a digital DA' , (see Figure 1) with a second order digital loop filter F(z) of the following type:

$$F(z) = A_1 + \frac{A_2}{.2\text{-}1} \tag{8}$$

where the A_1 and A_2 are the coefficients of the digital filter. For typical deep space missions, e.g. Mars Observer and Cassini, the coefficients are given by A_1 = 0.25 and A_2 = 0.03125. In order to use the analog results presented above, one must find the equivalent loop filter in the S-domain. The following section attempts to determine this equivalent loop filter.

3,2. Determining the Equivalent Loop Filter in the S-Domain

From Eq. (9), the loop filter F(z) in the discrete domain can be rewritten as

$$F(z) = K_f \left[\frac{1 - \gamma_2 z}{1 - \gamma_1 z} \right] \tag{9}$$

where

$$\gamma_1 = 1, \quad \gamma_2 = \frac{A_1}{K_f}, \quad K_f = A_1 - A_2 \tag{Io}$$

The goal is to find whether there exists appropriate values for τ_1 and τ_2 in Eq. (1) that can be used to approximate the digital loop filter in Eq. (9) so that the analog results presented in Section 3.1 can be applied, Using the Linear Interpolation Transformation (LIT) techniques [4], one can replace 1/s by

$$(T/2)\left[\frac{z+1}{z-1} \right]$$

into Eq. (1) to get an approximated digital loop filter for F(z), $F_{Ap}(z)$. Let a_1 and a_2 be defined as

$$a_1 = \frac{2\tau_1}{T} \tag{12}$$

$$a_2 = \frac{2\tau_2}{T} \tag{13}$$

then the approximated digital loop filter $F_{Ap}(z)$ of F(z) using LIT transformation technique can be written in terms of a_1 and a_2 as

$$F_{Ap}(z) = \left(\frac{a_2 - 1}{a_1 - 1}\right) \frac{\left|1 - \left(\frac{a_2 + 1}{a_2 - 1}\right) z\right|}{\left|1 - \left(\frac{a_1 + 1}{a_1 - 1}\right) z\right|} \tag{14}$$

Note that T is the nominal sampling period. For typical deep space missions, the nominal sampling period is (8 xl 03)-' sec.

Next, one would want to map Eq. (14) into Eq (9). By equating the coefficients between Eqs. (14) and (9), one obtains the appropriate time constants τ_1 and τ_2 for the corresponding analog filter that represents F(z) in the s-domain, namely,

$$\tau_1 = T\left[\frac{1}{K_f(\gamma_2 - 1)} + \frac{1}{2}\right] \tag{15}$$

$$\tau_2 = \frac{T}{2}\left[\frac{\gamma_2 + 1}{\gamma_2 - 1}\right] \tag{16}$$

Since one wants the approximated second order digital loop filter $F_{AP}(z)$ to be the same as F(z) described in Eq. (9), the values τ_1 and τ_2 calculated from Eqs. (15) and (16) must be selected in such a way that the following condition is satisfied

$$\gamma_1 = \left(\frac{a_1 + 1}{a_1 - 1}\right) \approx 1 \qquad (17)$$

As an example, for typical deep space missions, one obtains:

$$\tau_1 = 4.0585x10^{-3}\text{sec}, \tau_2 = 9.3662587x10^{-4}\text{sec} \qquad (18)$$

Using the calculated values for τ_1 and τ_2 in Eq. (18), one wishes to verify the condition in Eq. (17). By substituting these values into Eq. (17) one gets γ_1 = 1.03, which is approximately equal to 1. Therefore, for deep space applications, using the time constants found in Eq. (1 8), one can approximate the discrete loop filter F(z) in Eq. (8) by Eq. (1) in the s-domain, Thus, using the LIT method, the approximated analog loop filter for the digital filter described by Eq. (8) is found to be:

$$F(s) = \frac{1 + (9.3662587x10^{-4})s}{1 + (4.05850x10^{-3})s} \qquad (19)$$

Since one wishes to find an approximated analog loop filter that has a form expressed by Eq. (1) (so that the results presented in Section 3.1 are applicable), one must determine whether or not the 1.11 method will provide a "good approximation" of the digital loop filter in the analog domain. It will be shown later that the tracking phase jitter calculated using the loop filter approximated by LIT method is in good agreement with the results obtained by computer simulation. However, for completeness, one needs to find the actual representation of the analog loop filter described in Eq. (1) in the z-domain. After getting the actual representation of Eq. (1) in the s-domain, one can then approximate the digital loop filter F(z) described in Eq. (9).

In order to preserve the transient response of the analog loop filter F(s) in the discrete domain, the actual representation of Eq. (1) in the z-domain can be derived by using IIT method, This is derived as follows. First, the impulse response f(t) of the analog loop filter is found by taking the inverse Laplace transform of F(s). The desired impulse response f(n) for the digital loop filter then can be found by sample F(t) at each sampling interval T, i.e., f(n) = f(t = nT). The actual loop filter, $F_{Ac}(z)$, in the discrete domain is found by taking the Z-transform of f(n), namely [5],

$$F_{AC}(z)=\frac{\alpha_0-\alpha_1 e^{-\alpha_2 T}-1}{1-z^{-1}e^{-\alpha_2 T}} \qquad (20)$$

where the parameters α_0, α_1 and α_2 are given by

$$\alpha_0=\frac{\tau_2+1}{\tau_1}, \quad \alpha_1=\frac{\tau_2}{\tau_1}, \quad \alpha_2=\frac{T}{\tau_1} \qquad (21)$$

To approximate the digital loop filter expressed by Eq. (9) in the analog domain one rewrites Eq. (9) as follows

$$F(z)=K_f\left[\frac{\gamma_2-z^{-1}}{1-z^{-1}}\right] \qquad (22)$$

where K_f and γ_2 are given by Eq. (1 O). By comparing the coefficients of Eqs. (20) and (22), one can determine the time constants τ_{1Ac} and τ_{2Ac} for the corresponding analog loop filter, $F_{Ac}(s)$, that represents an approximation using IIT transformation for the digital loop filter described by Eq. (9). Comparing the coefficients between Eqs. (20) and (22), one gets

$$\left(\frac{\tau_{2Ac}+1}{\tau_{1Ac}}-\frac{\tau_{2Ac}}{\tau_{1Ac}^2}\right)=\gamma_2 \tag{23}$$

and

$$e^{-\frac{T}{\tau_{1Ac}}}=1 \tag{24}$$

The solutions to Eqs. (23) and (24) should satisfy the constraint

$$\frac{\tau_{2Ac}}{\tau_{1Ac}}e^{\frac{-T}{\tau_{1Ac}}}=1 \tag{25}$$

Note that Eq. (20) is indeed a good approximation of Eq. (22) when the constraint described by Eq. (25) is satisfied. If one picks

$$\frac{T}{\tau_{1Ac}}=0.0009 \tag{26}$$

then Eq. (24) becomes

$$e^{-\frac{T}{\tau_{1Ac}}}=0.999\approx 1 \tag{27}$$

From Eqs. (23) and (26), one can solve for τ_{2Ac} in terms of the sampling time T and γ_2

$$\tau_{2Ac}=\frac{e^{\frac{T}{0.0009}}-1}{1-\frac{T}{(0.0009)}} \tag{2s}$$

where the time constants τ_{1Ac} and τ_{2Ac} selected by Eqs. (26) and (28) should satisfy the constraint described in Eq. (25). If the selected time constants do not satisfy Eq. (25), one has to reselect a value for the ratio (T/τ_{1Ac}) and repeat the procedure again. For

instance, the calculated time constants for typical deep space applications are, from Eqs. (26) and (28),

$$\tau_{1Ac}=0.13889 \text{ sec}, \quad \tau_{2Ac}=0.13569 \text{ sec}. \tag{29}$$

Using these time constants one needs to verify the constraint dictated by Eq. (25), Substituting Eq. (29) into Eq. (25) one gets

$$\frac{\tau_{2Ac}}{\tau_{1Ac}} e^{\frac{-T}{\tau_{1Ac}}}=0.9778 \approx 1 \tag{30}$$

Hence, the calculated time constants expressed in Eq. (29) can be used to represent the loop filter in the analog domain. Therefore, for the typical digital DAL employed by deep space spacecraft, the approximated analog loop filter for the digital filter described by Eq. (8) using the 111' method is found to be:

$$F_{Ac}(z) = \frac{1+(0.1_{3569})s}{1+(0.13889)s} \tag{31}$$

4. BER Performance

In this section one will assume that the bit tracking is perfect in the bit synchronizer. When the two-sided loop bandwidth of the digital DAL (or the analog Costas loop) is small relative to the in coming data rate, then the phase error ϕ can be considered to be constant for many bit periods. Under these conditions, the conditional error probability is given by [2]

$$P_e(\phi) = \frac{1}{2} erfc(\sqrt{R_s}\cos(\phi)) \tag{32}$$

The average error probability is then obtained by averaging Eq. (32) over the probability density function (pdf) $P(\phi)$ of the phase error [2]

$$P_{Ae} = \int_{-\pi/2}^{\pi/2} P_e(\phi) P(\phi) d\phi \tag{33}$$

Using Eq. (33), one can derive the average Bit Error Rate (BER) performance for the digital DAL, the Costas loop with matched filter and clock feed back in the arm filter, and the Costas loop with second order Butterworth filter in the arm filter.

4.1 Digital DAL Loop

For digital DAL operates at high bit SNR ($R_s > 4$ dB) and small phase error ($\phi < \pi/12$), using Reference [2], the pdf for the phase error can be shown to have the following form

$$P(\phi) = \frac{e^{\alpha\cos(\phi)}}{\int_{-\pi/2}^{\pi/2} e^{\alpha\cos(\phi)} d\phi} \tag{34}$$

where

$$\alpha = \frac{1}{\sigma_\phi^2} \tag{35}$$

and σ_ϕ^2 is given by Eq. (2). By substituting Eq. (34) into Eq. (33) and evaluating the integral, one will obtain the average BER performance for the digital DAL loop.

4.2 Costas loop with Matched Filter and Clock Feed Back in (he Arm Filter

For this particular case, the passive arm filters of the Costas loop are replaced by the matched filter (integrate-and-dump type) with the clock feed back, When the transmitted data format is of NRZ type, the variance of the tracking phase error in the loop is found to be [3, Chapter 3]

$$\& \quad = \frac{1}{\rho_C S_L} - \tag{36}$$

where ρ_C and S_L are the loop SNR and the loop squaring loss, respectively. They are given by

$$\rho_C = R_s \delta \tag{37}$$

$$S_L = \frac{1}{1 + \frac{1}{2R_s}} \tag{38}$$

The pdf for the tracking phase error of the Costas loop is

$$P(\phi) = 2\frac{e^{\frac{\cos(2\phi)}{4\sigma_{\phi C}^2}}}{2\pi I_0\left(\frac{1}{4\sigma_{\phi C}^2}\right)}, \quad |\phi| \le \frac{\pi}{2} \tag{39}$$

Again, the average BER performance for this loop can be obtained by substituting Eq. (39) into Eq. (33) and evaluating the integral.

4.3 **Costas** loop with the Second **Order Butterworth Filter** in the **Arm Filter**

For this loop, the passive arm filters are second order Butterworth filters with B denotes the single-sided noise bandwidth of the filter. The pdf and the variance for the tracking phase error of this loop has the same forms as that of Eqs. (39) and (36), respectively. However, the squaring loss, S_L, of the loop becomes [3, Chapter 3]

$$S_L = \frac{K_1^2}{K_2 + K_L \frac{\eta}{R_s}} \tag{40}$$

where $K_L = 3/4$ for second order loop, and K_1, K_2 and η are given by

$$K_1 = 1 - \frac{1}{8\eta}[1 - e^{-4\eta}(\cos(4\eta) - \sin(4\eta))] \tag{41}$$

$$K_2 = 1 - \frac{1}{32\eta}(5 - [8\eta\cos(4\eta) + 5(\cos(4\eta) - \sin(4\eta))]e^{-4\eta}) \tag{42}$$

$$\eta = \frac{B}{R_s} \tag{43}$$

s. Numerical results

Using typical parameters for deep space missions, Figures 3 and 4 show the plots of the phase jitter for the second order digital DAL (see Eq. (2)) using the approximated loop filters described in Eqs (19) and (31). The approximated loop filters expressed in Eqs (19) and (31) were derived using LIT and IIT methods, respectively. The results obtained from the first order loop using linear approximation [2] are also presented for comparison. Figure 3 shows that the tracking phase jitter (obtained using LIT transformation technique) remains almost constant as one switches the data

rate from 7,8125 bps to 500 bps (corresponding to $B_L T_b$ = 0.1574 and $B_L T_b$ = 0.1566). Note that 7.8125 bps and 500 bps are the typical lower bound and upper bound, respectively, for the deep space telecommand data rate. The results are confirmed with the actual design and operation of the deep space spacecraft, e.g. Mars Observer and Cassini. On the other hand, Figure 4 shows that the phase jitter of the actual approximation does not remain constant as one switches the data rate. It is interesting to observe that the phase jitter approximated by using the IIT for 50'0 bps (corresponding to $B_L T_b$ = O. 1566) approaches that of the phase jitter obtained by using the linear first order approximation. While the phase jitter derived from the actual transformation for **7.8125** bps (corresponding to $B_L T_b$ = O. 1566) **is** approximately the same as the phase jitter derived from LIT method for the second order loop (see Figure 5,)

The second order digital DAL shown in Figure 1 has been implemented using a Signal processing Workstation (SPW) of Comdisco. Simulations have been run at $B_L T_b$ = 0.1566 and the simulation results are plotted in Figure 5 for comparison purpose. This figure shows that the simulation results are in good agreement with the analytical results derived by using LIT technique.

Using the phase jitter derived from the LIT method, the plot of BER performance for communications system using DAL (see Eq. (33) and (34)) is shown in Figure 6. The results for the first order loop is also illustrated in this figure for comparison purpose. Figure 6 shows that the average BER performance is nearly the same when

one switches the data rate from 7.8125 bps to 500 bps, In addition, this figure also shows that the average BER performance for the first order loop is almost the same as that of the second order loop. The BER degradation due to the ph ıse jitter for the second order loop is about 0.1 dB for all practical cases of interest, e., BER = 10^{-3}-10-8.

Figure 7 compares the average BER performance between the digital DAL and Costas loops. Performances of the Costas loop with second order Butterworth filter in the arm filter and the Costas loop with matched filter and clock feed back in the arm filter are shown in this figure, This figure clearly demonstrates the superiority performance of the communications system employing digital DAL.

6. Conclusion

A thorough investigation of the second order digital suppressed-carrier DAL has been presented in this paper. The mathematical models for the tracking phase jitter and the BER performance have been derived from the analog, results presented in [1].

To characterize the behavior of the tracking phase jitter of the second order digital DAL using available analog results, both IIT and LIT methods have been applied to the approximations of the digital loop filter. The analytical results obtained from these transformation techniques are then compared with the computer simulation results. The comparison reveals that the results obtained by the LIT technique are in good agreement with computer simulation results. In addition, the analytical results also show that the tracking phase jitter remains almost constant when there exists a

small deviation in $B_L T_b$. Note that a small deviation in $B_L T_b$ can occur when one switches the data rate. Therefore, the analytical model employing the LIT method can be used to predict the behavior of the tracking phase jitter of the second order digital DAL for all data rates.

Using the derived tracking phase jitter, we can determine the BER performance of the second order digital suppressed-carrier DAL. It has been found that, for typical space applications, the BER degradation due to the tracking phase jitter for the second order digital DAL is about 0.1 dB for BER = 10-3-10-8. Furthermore, it has been shown that the digital DAL outperforms the commonly used Costas loops such as Costas loop with second order loop filter in the arm filter or Costas loop with matched filter and clock feed back in the arm filter.

The numerical results presented in this paper are shown for typical deep space communications sytems. However, the performance evaluation technique proposed here can easily be generalized to evaluate other communications systems that employ digital DAL for their carrier (or subcarrier) tracking.

Acknowledgement

The author is indebted to D. Hansen for providing the computer simulation results presented in Figure 5, S. Hinedi for his comments and suggestions during the preliminary review of this work, and A. Kermode, B. Charny and C. Kyriacou for their constant support and encouragement. The work described in this paper was carried out at the Jet Propulsion Laboratory, California Institute of Technology, under contract with the National Aeronautics and Space Administration.

References

[1] Lindsey, W. C., M. K. Simon, "Data-Aided Carrier Tracking Loops," IEEE Transactions on Communications Technology, Vol. COM-19, No. 2, April 1971, pp. 157-168.

[2] M, K. Simon, J. C. Springett, "The Theory, Design, and Operation of the Suppressed Carrier Data-Aided Tracking Receiver," Technical Report 32-1583, June 15, 1973, Jet Propulsion Laboratory, California.

[3] J. Yuen, "Deep Space Telecommunications Systems Engineering," Plenum, New York, 1983,

[4] E.I. Jury, Theory and Application of the Z-Transform Method, Chapter 7, John Wiley & Son, Florida, 1986.

[5] J. W. Heller, "A Digital Filter Implementation of the Deep Space Tran spender PLL Integrator," TDA Progress Report 42-66, September-October 1981, Jet Propulsion Laboratory, California.

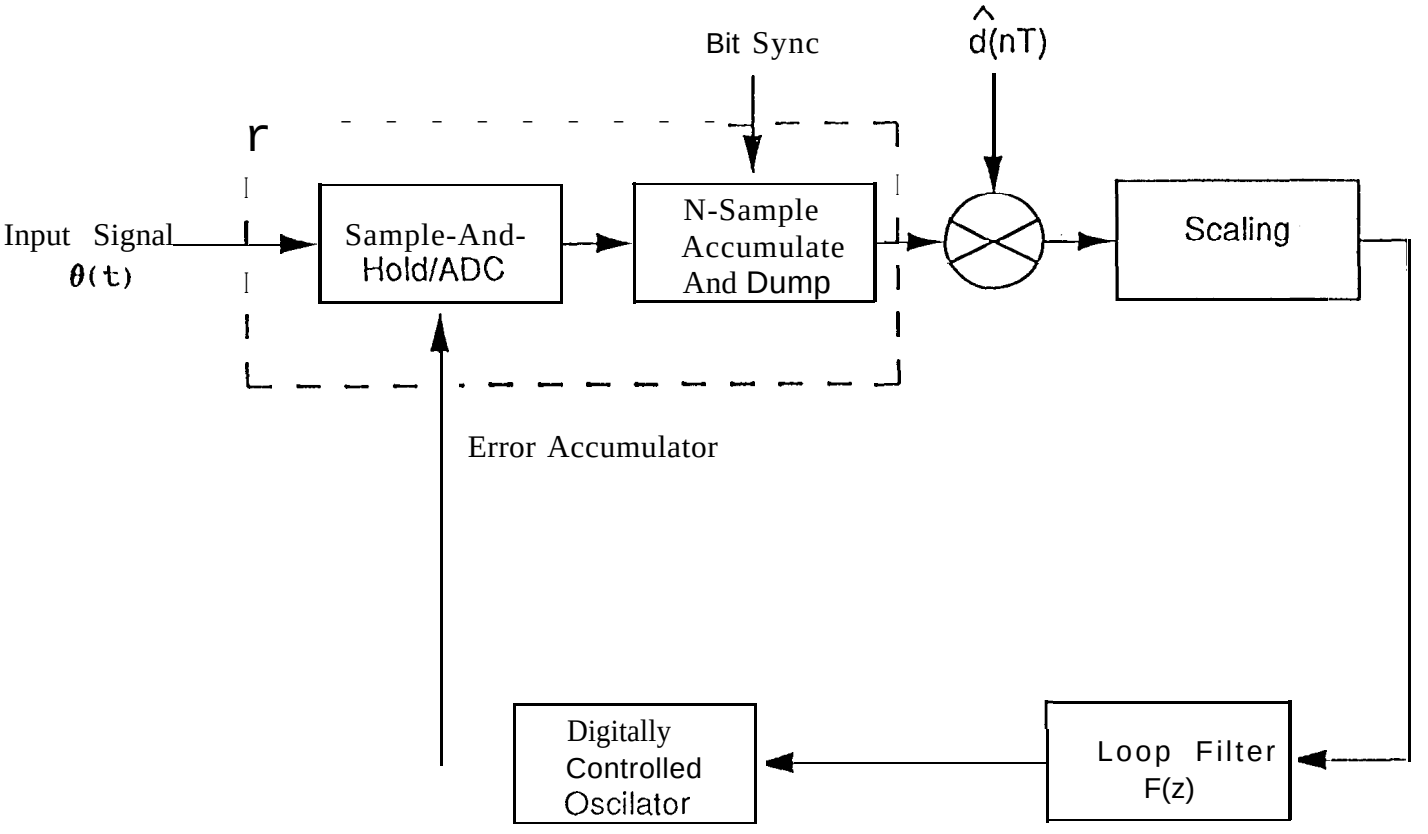

Figure 1 Simplified Block Diagram for the Digital Data-Aided Loop

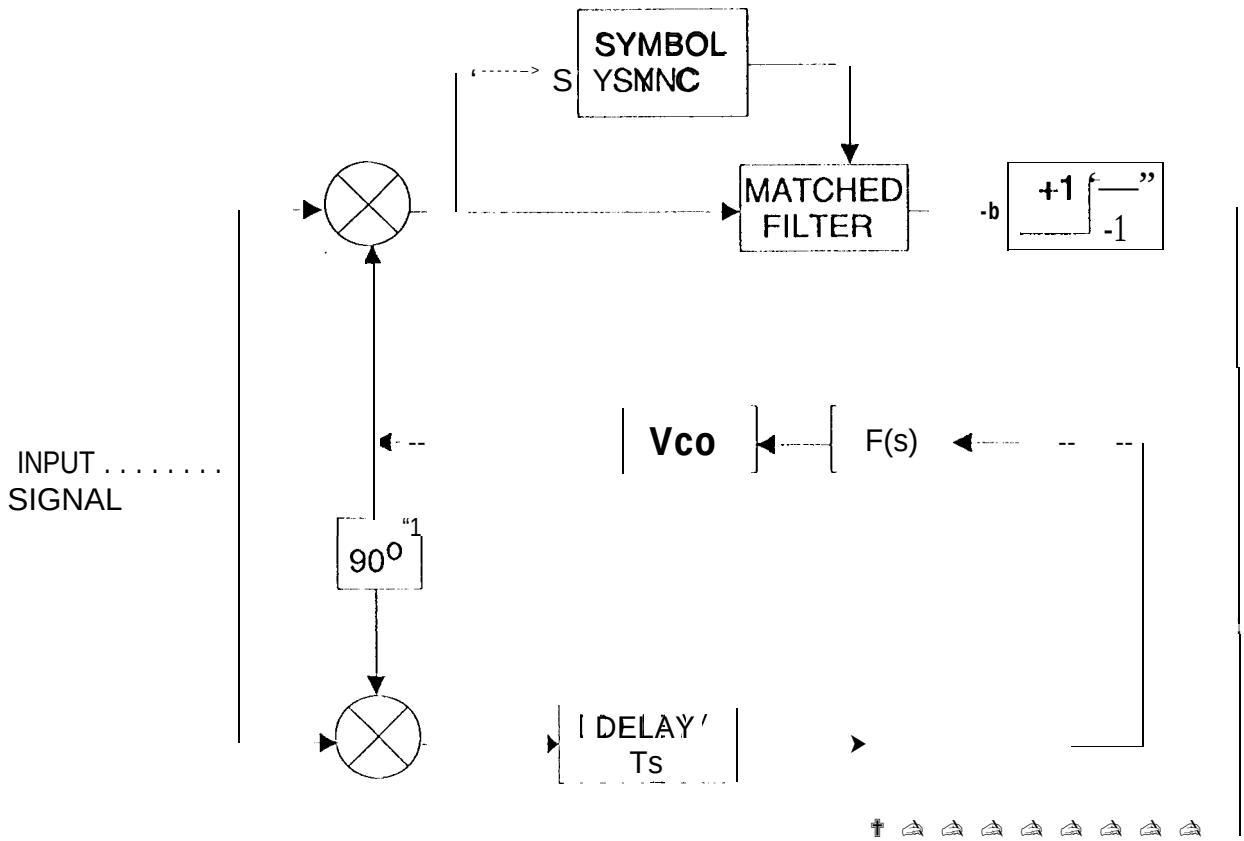

FIGURE 2 . Simplified Block Diagram for the Analog Data-Aided Loop

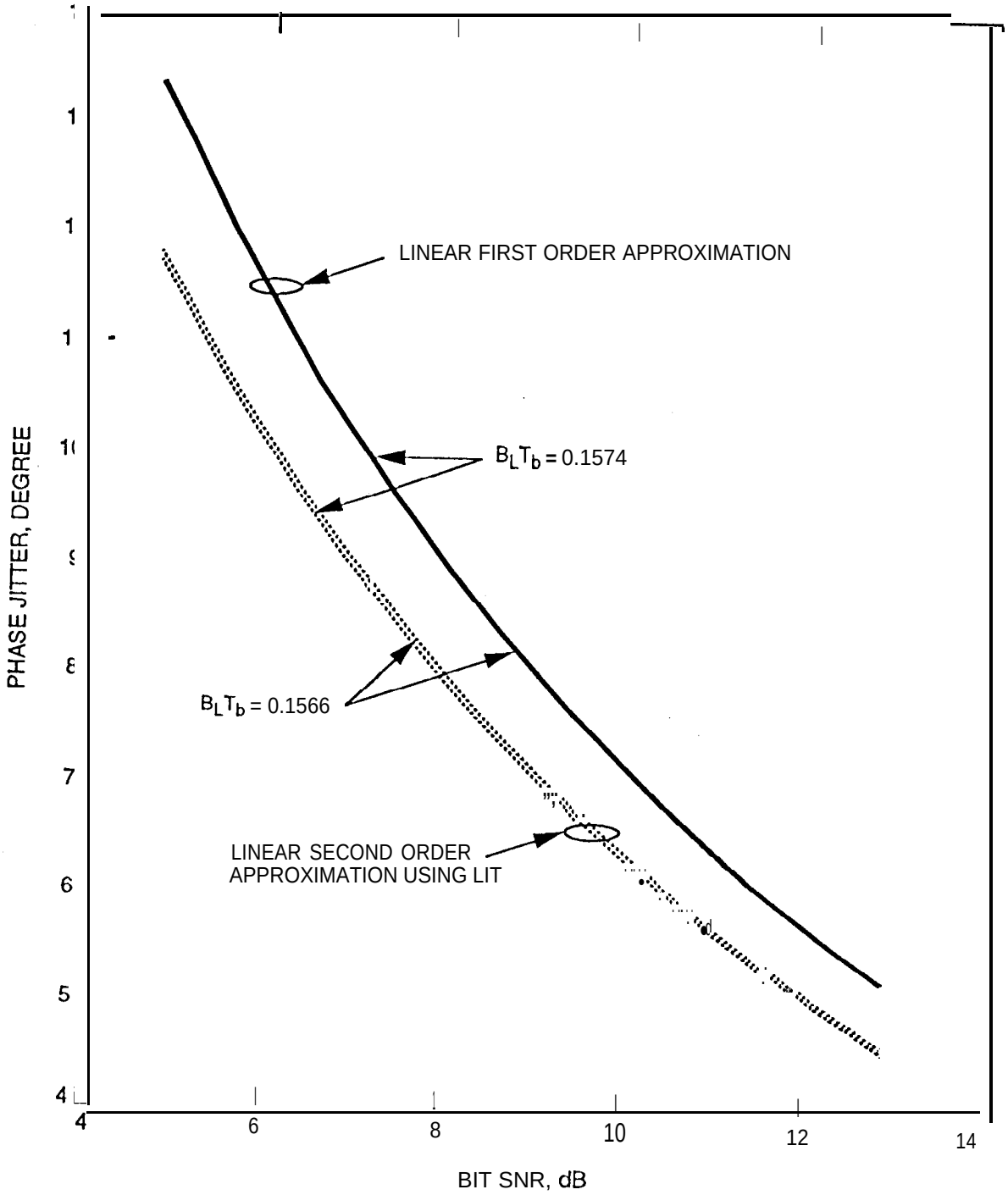

Figure 3. Phase Jitter Using L.I.T.

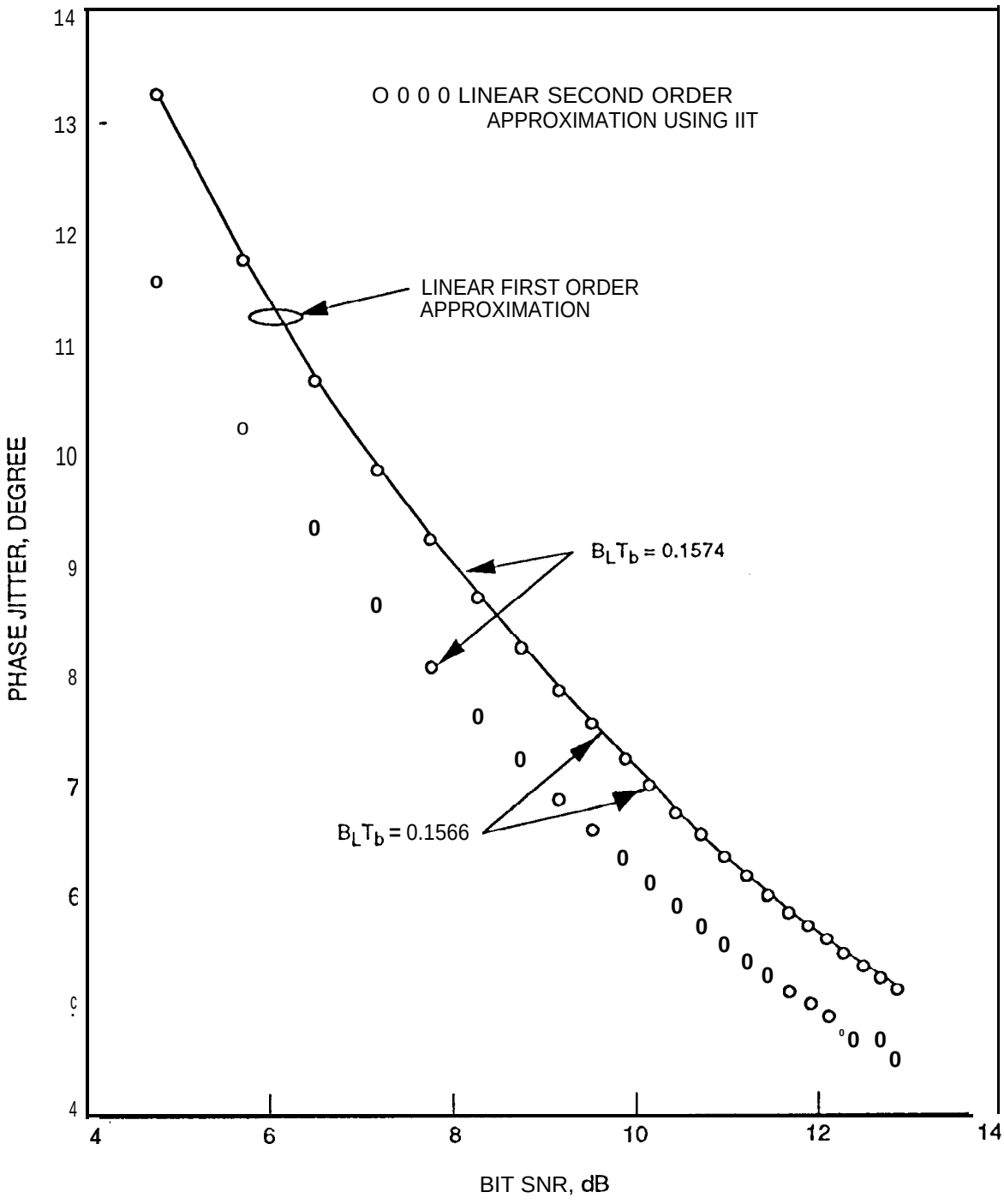

Figure 4. Phase Jitter Using IIT

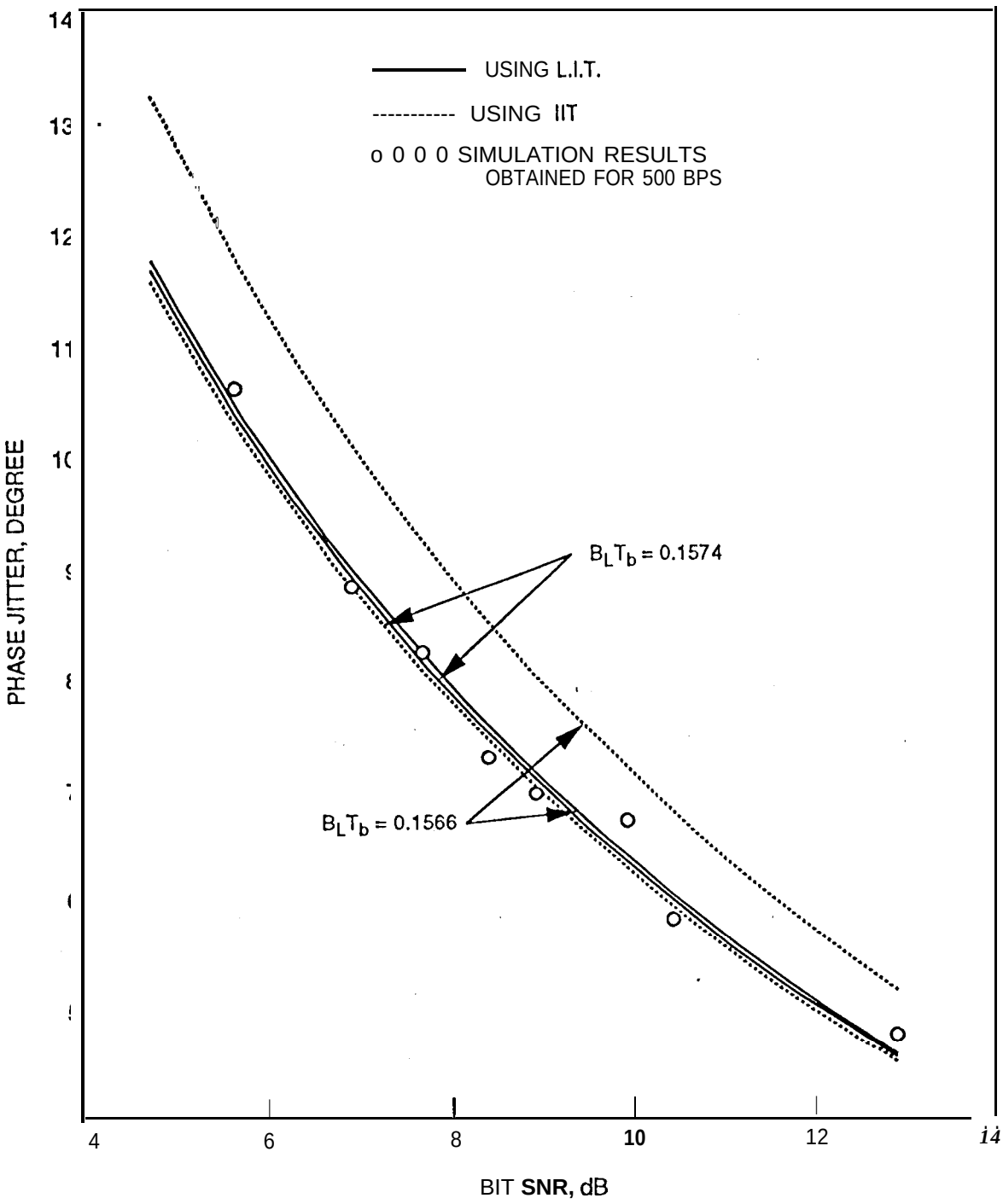

Figure 5. A Comparison Between IIT and L.I.T.

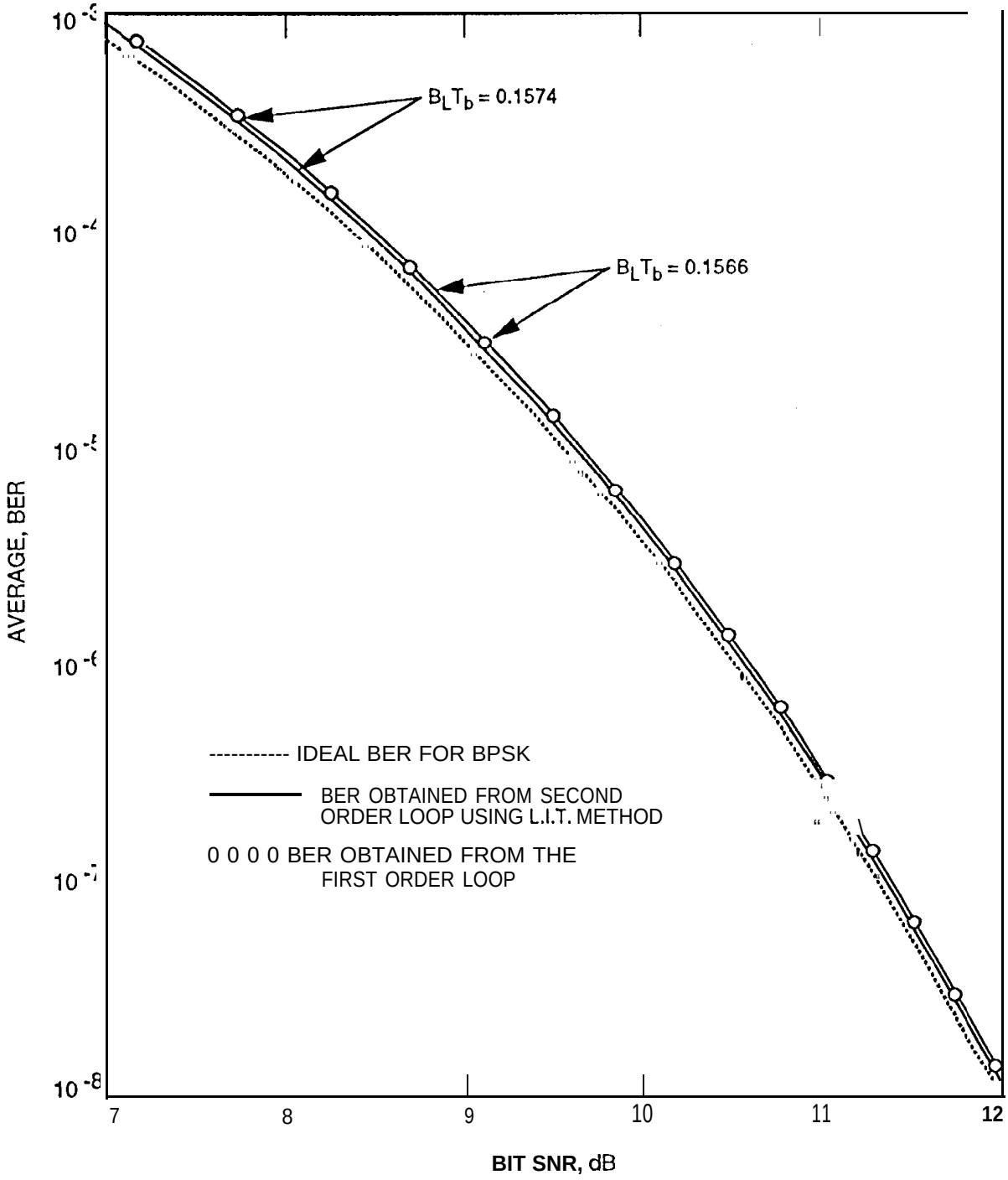

Figure 6. BER Performance for Digital DAL

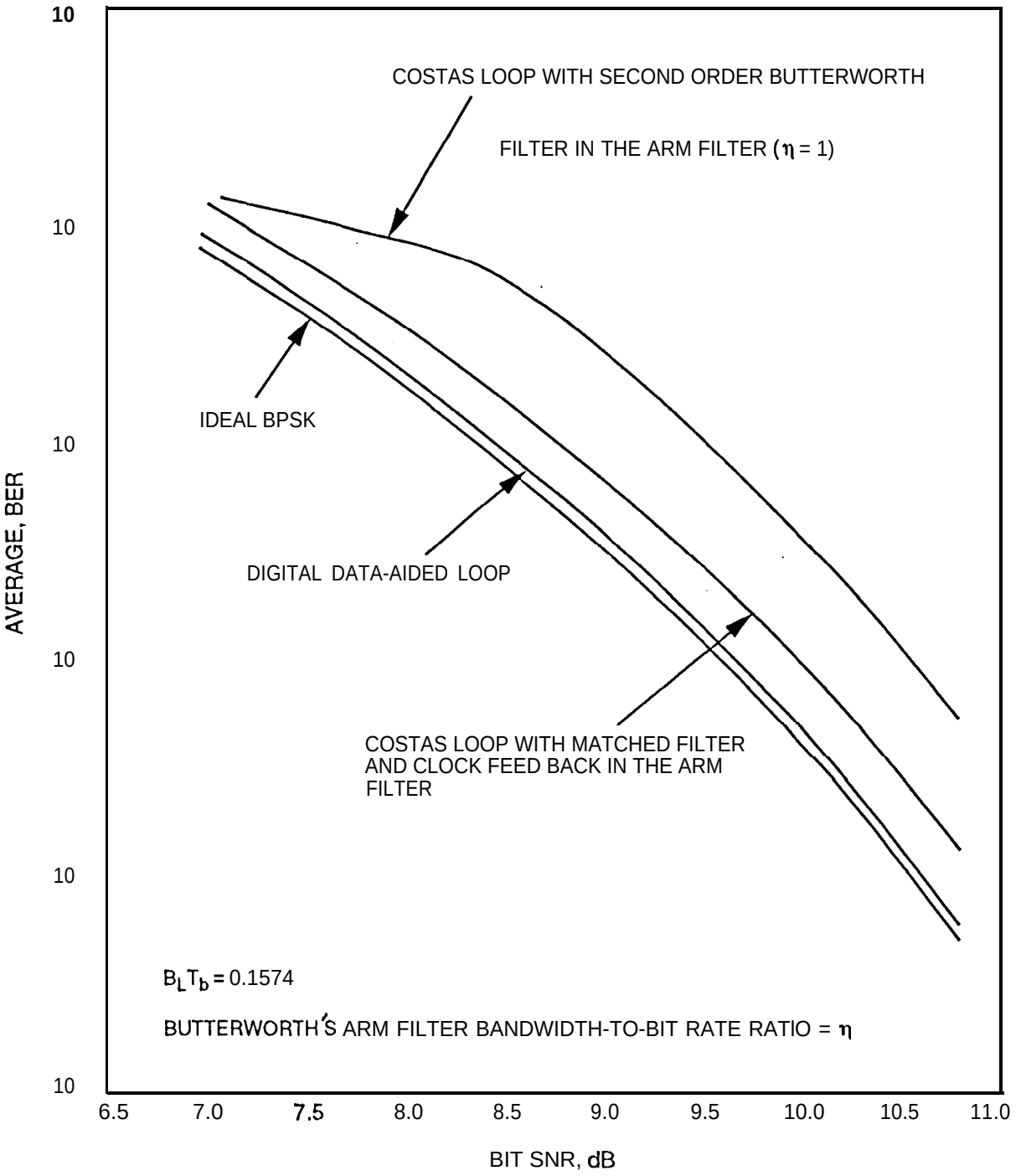

Figure 7. Average Probability of Error for Digital DAL and Costas Loop